A COUPLED MODEL FOR NATURAL CONVECTION AND CONDENSATION IN HEATED SUBSURFACE ENCLOSURES EMBEDDED IN FRACTURED ROCK

Halecky, N.[1+3], J.T. Birkholzer[1], S. W. Webb[2], P. F. Peterson[3], G.S. Bodvarsson[1]

[1]Lawrence Berkeley National Laboratory, Berkeley, CA
[2]Sandia National Laboratories, Albuquerque, NM
[3]University of California at Berkeley, Berkeley, CA
e-mail: nehalecky@lbl.gov

ABSTRACT

In heated tunnels such as those designated for emplacement of radioactive waste at Yucca Mountain, axial temperature gradients may cause natural convection processes that can significantly influence the moisture conditions in the tunnels and in the surrounding fractured rock. Large-scale convection cells would provide an effective mechanism for axial vapor transport, driving moisture out of the formation away from the heated tunnel section into cool end sections (where no waste is emplaced). To study such processes, we have developed and applied an enhanced version of TOUGH2 (Pruess et al., 1999) adding a new module that solves for natural convection in open cavities. The new TOUGH2 simulator simultaneously handles (1) the flow and energy transport processes in the fractured rock; (2) the flow and energy transport processes in the cavity; and (3) the heat and mass exchange at the rock-cavity interface. The new module is applied to simulate the future thermal-hydrological (TH) conditions within and near a representative waste emplacement tunnel at Yucca Mountain. Particular focus is on the potential for condensation along the emplacement section, a possible result of heat output differences between individual waste packages.

INTRODUCTION

Extensive scientific investigations have been conducted at Yucca Mountain, Nevada, to explore whether the site is suitable for geologic disposal of radioactive waste. The heat produced by the radioactive waste will significantly change the thermal and hydrological environment at Yucca Mountain, affecting both the host rock and the conditions in the tunnels. Pore-water vaporization and subsequent condensation will lead to a large saturation and flux redistribution in the near-field fractured rock. Also, as vapor enters the emplacement tunnels (drifts), the vapor concentration near waste packages will increase. Understanding these changes—in both the natural system and the drifts—is essential for evaluating the future performance of the repository in terms of canister corrosion and radionuclide containment.

The thermally driven flow processes to be expected in the fractured rock at Yucca Mountain have been investigated in various modeling studies (e.g., Haukwa et al., 2003; Birkholzer et al., 2004). Gas flow along emplacement drifts has usually been neglected in these models, either because individual drifts were not represented at all or were treated as closed systems without axial flow and transport components. As a result, the models predict that the majority of the vapor produced from boiling/ evaporation of formation water remains in the fractured rock. Simulations presented in this paper show that there may be considerable vapor transport from the fractured formation into the emplacement drifts. Recent CFD (computational fluid dynamics) simulations suggest that large-scale axial convection cells would form within emplacement drifts (Webb and Itamura, 2004; Webb and Reed, 2004), providing an important transport mechanism that can move vapor away from the vapor-producing sections to the cold end of the drifts.

In this paper, we describe a new simulation method that simultaneously handles mass and heat transport in the fractured formation *and* in the emplacement drifts. The model concepts used for the partially saturated fractured rock are based on existing TOUGH2 models as described, for example, in Haukwa et al. (2003) and Birkholzer et al. (2004). Using a newly developed TOUGH2 module, in-drift natural convection is approximated as a binary diffusion process, with effective mass dispersion coefficients estimated from supporting CFD analyses described in Webb and Itamura (2004) and Webb and Reed (2004). In previous analyses (Birkholzer et al., 2005, 2006), the new simulation method was applied to better understand how natural convection in Yucca Mountain drifts would affect the near-drift TH processes, particularly with respect to the saturation changes and flux perturbations in the fractured rock. In this paper, we conduct similar analyses, but focus on the potential for in-drift condensation as triggered by the considerable heat output differences between individual waste packages. Our three-dimensional model domain comprises one representative drift and the surrounding fractured rock, with two 40 m long drift sections discretized in detail such that the heat output of individual waste packages can be simulated.

BASIC TH PROCESSES

At Yucca Mountain, the heat emanating from the waste packages (horizontally emplaced cylindrical canisters about 5 m long, with a small gap in between them) will be effectively transferred to the drift walls, mostly via thermal radiation. At early stages after emplacement, temperatures in the partially saturated formation near the drifts will heat up to above-boiling conditions. As a result, the initially mostly stagnant pore water in the rock matrix will become mobile through boiling (see Figure 1a). Vaporization causes a pressure increase, which will drive the vapor away from the boiling region, both into more distant rock regions (where the vapor will condense and enhance liquid fluxes) as well as into the drifts. At later times, when temperatures decreases below boiling, the rock mass near the drifts will gradually rewet (Figure 1b).
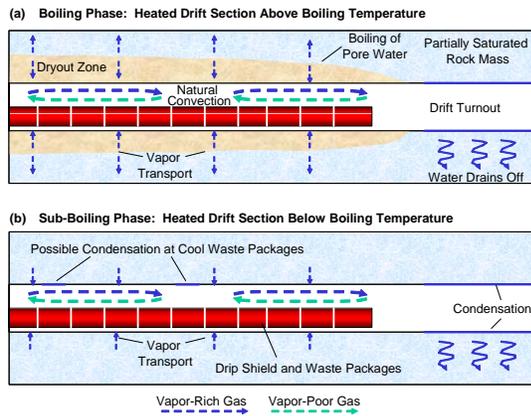

Figure 1. Schematic of expected TH processes along emplacement drift with individual waste packages (modified from Webb and Reed, 2004).

Vapor entering the emplacement drifts from the fractured porous rock is subject to effective radial and axial mixing transport as a result of natural convection processes. Axial mixing can reduce the overall moisture content in heated drift sections because of the presence of the unheated drift ends (turnouts). Principles of thermodynamics suggest that the maximum amount of vapor that can be present in air decreases with declining temperature. Thus, the warm vapor-rich gases moving from heated drift sections toward the drift turnouts—caused by natural convection processes—will be depleted of most of their vapor content through condensation on cooler rock surfaces. This will cause a local pressure sink, which may further the axial gas transport. (Note that the condensate will drain away from the repository into underlying rock units.) At the same time, vapor-poor gas will circulate towards the emplacement sections of the drifts, thereby reducing the moisture content in these areas (Birkholzer et al., 2005, 2006).

While most of the condensation is expected to occur in the unheated drift turnouts, temperature variation between individual waste packages may also cause local condensation along the heated drift section (Figure 1b). The potential for and the magnitude of local condensation depends on the average moisture content in the heated drifts in conjunction with local temperature and relative humidity variability.

MODELING APPROACH

Modeling Framework for Fractured Rock Mass

The modeling framework for simulating the TH conditions in the near-field fractured rock is adopted from existing TH models for Yucca Mountain (e.g., Haukwa et al., 2003; Birkholzer et al., 2004). The TOUGH2-EOS4 simulator (Pruess et al., 1999) accounts for convective and diffusive movement of gaseous and liquid phases of components water and air (under pressure, viscous, capillary, and gravity forces); transport of latent and sensible heat; phase transition between liquid and vapor; and vapor pressure lowering. The fractured rock is described using a dual permeability concept, assuming two separate but interacting continua that superpose with each other in space. One continuum describes flow and transport in the fractures; the other describes flow and transport in the rock matrix.

Modeling Framework for Emplacement Drifts

In principle, the mass and heat transport processes occurring in an open drift could be modeled with a CFD simulator that would solve the mass, momentum, and energy conservation equations, including their turbulent contributions (e.g., Webb and Itamura, 2004; Webb and Reed, 2004). However, solving the turbulent velocity fields expected in heated drift sections would require fine spatial and temporal resolution. Not only would this result in highly time-consuming simulation runs, but would also necessitate complex coupling approaches, because of the large discretization disparities between the drift and the fractured rock.

For the purpose of this study, we follow the methodology described in Webb and Itamura (2004), and assume that the axial transport of vapor and air can be simplified as a binary diffusion process of the air-vapor mixture, using effective mass dispersion coefficients calculated from complementary CFD flow field simulations. By approximating natural convection as a binary diffusion process, the in-drift heat and fluid flow processes can, in principle, be simulated with the standard methodologies applied for Darcy-type flow and transport (such as those implemented in TOUGH2), with the drift represented as a specific solution subdomain that requires certain code modifications and parameter specifications. A new drift simulation version of TOUGH2 was developed

that can solve simultaneously for heat and fluid flow within the drift and in the surrounding rock mass (Birkholzer et al., 2005, 2006). The following code modifications were made:

- Users may define natural-convection subdomains in which binary diffusion is calculated using predescribed values for the effective mass dispersion coefficients. For simplification, the coefficients are assumed to be identical in axial and radial direction.

- The heat and mass transfer between the gas flow in the natural-convection subdomain and the near-drift fractured rock is calculated from empirical boundary-layer correlations given in the literature. This transfer is affected by the presence of a surficial fluid boundary layer, where the motion of particles is retarded compared to the free stream velocity. Different correlation models have been implemented in the new TOUGH2 version. The correlations used in this study were derived for free convection in the annular space between horizontal eccentric cylinders, which roughly represents the geometry of an open drift with a drip shield/waste package assembly. See details in Webb and Reed (2004) and Birkholzer et al. (2005).

- The new TOUGH2 version allows for the definition of radiation-only connections, where all other heat and mass transport processes are eliminated. Users can define direct radiative connections between emitting (waste packages) and receiving surfaces (drift wall, invert) across open gas spaces that are finely discretized to allow for in-drift mass and heat transfer. Similar to the standard TOUGH2, radiation is described with the Stefan-Boltzmann equation (Pruess et al., 1999). A new preprocessing code was developed that calculates three-dimensional view factors for a detailed representation of radial and axial surface-to-surface radiation (see Figure 3).

Model Setup

Three-dimensional simulations runs were performed for a simplified geometrical representation of an emplacement drift located in one of the southern panels of the repository. The model domain comprises the entire unsaturated zone, having the ground surface as the upper model boundary and the groundwater table as the lower model boundary. In axial drift direction (y-direction), symmetry allows for reducing the model to half of the drift length. Thus, the simulated drift comprises half of the typical emplacement section length (300 m), followed by a 80-m unheated section away from the symmetry axis. The total length of the model domain in y-direction is 520 m. Symmetry assumptions can also be used to reduce the model domain in the x-direction, perpendicular to the drift axis. The current repository design of parallel drifts can be represented as a series of symmetrical, identical half-drift domains with vertical no-flow boundaries between them. Thus, the numerical mesh can be limited to a lateral width of 40.5 m, extending from the drift center to the midpoint between drifts.

The three-dimensional grid used in the simulations comprises about 14,000 finite volumes with about 50,000 connections. Figure 2 shows the grid in a vertical cross section orthogonal to the drift axis (x-axis). Focusing on in-drift and near-drift conditions, it is important to represent the drift and its vicinity with a refined discretization. Simplifications are necessary, on the other hand, to ensure that the simulation effort is not excessive. For example, the waste package, the drip shield, and the small air space between them are treated in our study as a lumped entity in the simulation runs with equivalent thermal properties (based on averaging the respective thermal properties of the waste package, drip shield, and air). Thus, the flow and transport processes occurring under the drip shield and in the gap between waste packages are neglected in this study.

As shown in Figure 3, the numerical grid comprises various vertical slices of varying thickness along the drift axis (y-axis), ranging from less than 5 m to about 80 m. Similar to BSC (2005), there are two finely gridded segments along the emplacement section of the drift—one near the drift center, the other at the end of the emplacement section—where the thickness of the vertical slices corresponds to the axial length of individual waste packages. Only in these segments is the strong heat output variability between waste packages taken into account; i.e., the potential for local condensation can be evaluated. Waste packages are arranged in sequence according to an idealized design option described in BSC (2003), with a cool waste package such as the "5 HLW" situated next to hotter waste packages such as the "21 PWR" or the "44 BWR" (Figure 3). For grid efficiency purposes, all other emplacement regions have the decay heat imposed as a uniform axial line load.

The thermal load of all waste packages is time-dependent (Figure 4), exponentially decaying from an initial value that ranges between 0.2 kW (for the "5 HLW LONG") and 2.3 kW per meter drift length (for the "21 PWR"). For comparison: the initial value for an average thermal line load (TLL) is 1.45 kW/m. Note that a considerable amount of the decay heat is removed by forced drift ventilation during the first 50 years after emplacement (preclosure period). Similar to previous studies (e.g., Haukwa et al., 2003; Birkholzer et al., 2004), forced drift ventilation is not explicitly modeled in our simulation. Rather, the heat losses by forced drift ventilation are incorporated by reducing the effective heat output in the simulation to about 14% of its original value, based on design estimates (BSC, 2004).
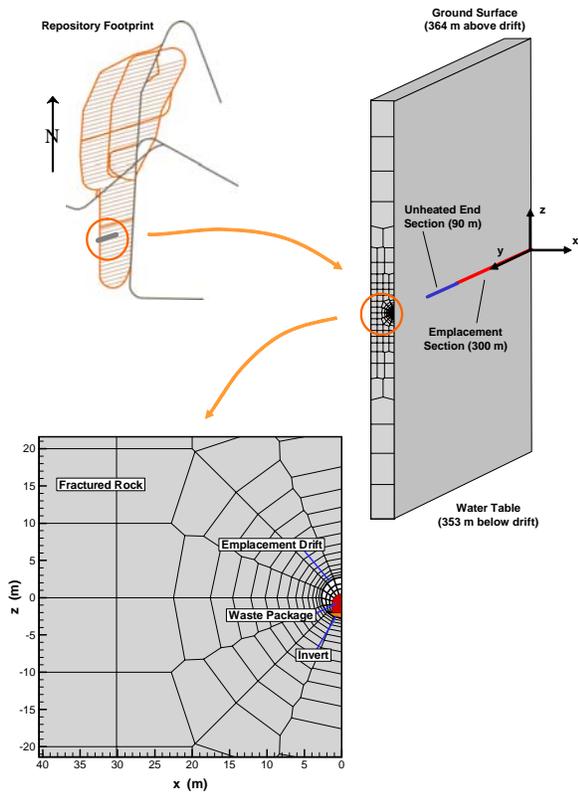
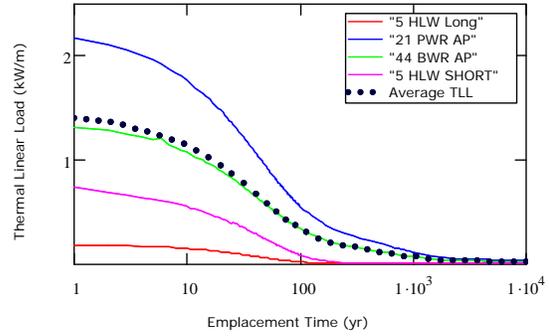*Figure 2. Schematic showing geometry of 3D model domain (not to scale).*

Figure 4. Thermal load of individual waste packages as a function of time. "Average TLL" is average thermal line load.

As pointed out before, natural convection is treated as a binary diffusion process in this study, with effective diffusion coefficients derived from CFD studies. There is, however, considerable uncertainty as to the magnitude of these coefficients. Two vastly differing sets of dispersion values were derived in Webb and Itamura (2004), representing first-order estimates for the possible range of natural convection conditions in Yucca Mountain drifts (see Table 1). To account for this uncertainty, we run two main simulation cases, one with strong convective mixing (Case 1), the second with moderate convective mixing (Case 2). All other material properties and the model boundary conditions are described elsewhere (e.g., Birkholzer et al., 2005), and shall not be repeated here.
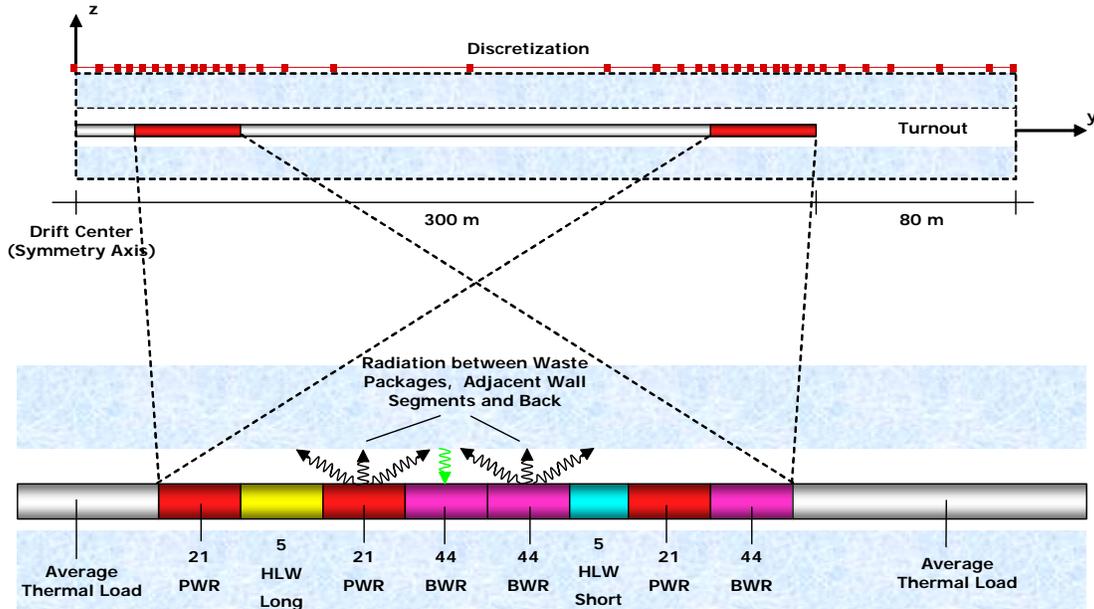

Figure 3. Schematic model geometry along emplacement drift. Red dots indicate location of vertical slices. Two segments are finely discretized to accompany individual waste packages. Notice the yellow and cyan "HLW" waste packages, which have the smallest decay heat.

Table 1: Mass dispersion coefficients (m²/s)

Cases/Time Period (years)	300 - 600	600 - 2000
Case 1: Strong convective mixing	0.1	0.1
Case 2: Moderate convective mixing	0.008	0.004

MODEL RESULTS

Our aim in this paper is to evaluate the potential of local condensation in drift segment containing comparably cool waste packages. Condensation can only occur when the local temperature drops below the boiling point of water. Previous experience with similar models has shown that this occurs between 600 and 1000 years after waste emplacement (Birkholzer et al., 2005, 2006). Therefore our model simulations were run until 2000 years after emplacement to ensure sub-boiling conditions occurred in every waste package. In lieu of the primary interest of the study, we will focus in our discussion on the TH conditions within the drifts, and refer to previous papers (Birkholzer et al., 2005, 2006) for a detailed analysis of the TH conditions in the near-field fractured rock mass.

First, let us examine the temperature response in the drift as a function of time. Figure 5 shows profiles along the drift crown, for Case 1 with strong convective mixing and Case 2 with moderate convective mixing. Note that in this figure, and all other profile plots to follow, the distance along the drift is measured from the center of the heated section of the drift, the symmetry boundary of the half-drift model. The heated section of the drift ends at 300 m (indicated by dashed vertical line), followed by the 80 m long unheated end section.

In both cases, the emplacement section of the drift heats up strongly to about 140°C at 100 years after waste emplacement. As discussed previously in section "Basic TH Processes", this temperature increase causes boiling of pore water in the adjacent rock mass combined with significant vapor transport into and along the heated drift. The temperature trend reverses at later stages, when the reduced heat output of the radioactive waste (see Figure 4) results in a gradual temperature decrease. At 500 years, for example, the in-drift temperatures have reduced to a few degrees centigrade above boiling along most of the heated section. At later times, between 500 and 1000 years, the entire heated section of the drift drops completely below the boiling temperature, creating the potential for water vapor to condense near the waste packages. However, all temperature profiles, even at 2000 years after emplacement, remain elevated from ambient temperature, and exhibit

moderate to strong temperature differences between the heated drift section and the unheated end (indicating that natural convection processes will still be relevant even at these later times).

We observe that the varying heat output of the individual waste packages causes strong temperature differences between neighboring drift crown segments. At 100 years, these differences are larger than 5°C near the "5 HLW Long" waste packages, which have the smallest thermal load, and a little less than 5°C near the "5 HLW Short" waste packages, which have the second-smallest thermal load (see Figures 3 and 4). Even at 1000 years, when the drift crown temperature has dropped below boiling, there exists a roughly 2°C difference between the "21 PWR AP" and the "5 HLW Long" waste packages for both simulation cases. With this temperature difference occurring over a short distance of 5 m, areas near the cool waste package might act as a "cold traps" for water vapor to condense.

Overall, the temperature differences between Case 1 and Case 2 are rather subtle, indicating that the transport of sensible and latent heat with the gas flow in the drift is not overly important for the in-drift temperature distribution. The temperatures for the case with strong convective mixing are slightly lower in the heated section and slightly higher in the end section of the drift, a result of the more effective convective heat transport in axial direction.
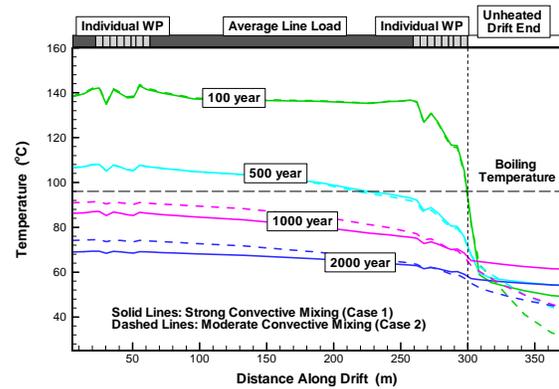

Figure 5. Temperature along drift crown for Case 1 (solid lines) and Case 2 (dashed lines)

In Figure 6, we evaluate the temporal evolution of vapor concentration (calculated as mass fraction of vapor in the gas phase) along the drifts for the two simulation cases. As mentioned before, Case 2 differs from Case 1 in that the convective mixing between vapor-rich heated section and the vapor-poor end section of the drift is less effective. As a result, the amount of vapor in the emplacement section is much higher in Case 2 at all times, with maximum vapor concentrations of about 0.9 at 100 years. In Case 1 the vapor mass fraction in the gas phase is never

above 0.4, even at early times when significant amounts of vapor are produced from pore water boiling. Even with the large temperature differences between neighboring waste packages observed in Figure 5, the gas in the open drift appears well mixed enough, in both cases, to allow for smooth vapor concentration profiles along the drift length.
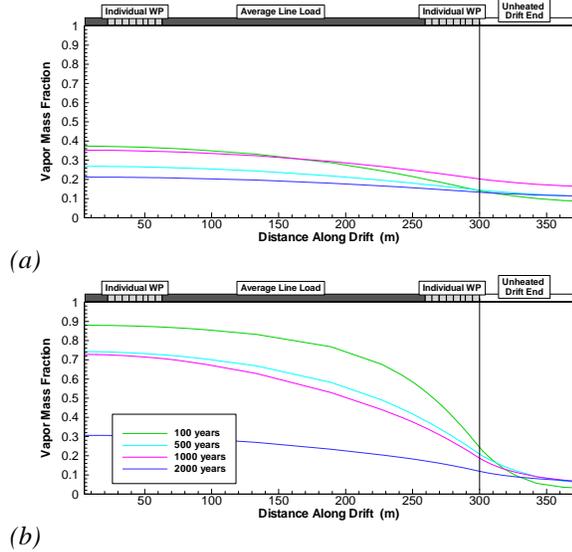

(a)

(b)

Figure 6. Vapor Mass Fraction along drift crown for (a) Case 1 and (b) Case 2.

Condensation of water vapor occurs when the gas reaches specific thermodynamic conditions, namely a pressure and temperature state, where it is unable to contain any more water in the gas phase. The relative humidity, a ratio of the actual vapor pressure to the saturated vapor pressure, is an indicator of when these conditions for condensation exist. When the relative humidity of a gas is at 100%, any additional water vapor introduced must condense to liquid. To understand these effects on the in-drift environment in more detail, we compare the relative humidity of the gas at the drift crown along the length of the drift for both the strong and moderate convective mixing cases, as shown in Figure 7.

Independent of the simulation case, all relative humidity profiles exhibit relative humidities of 100% in the unheated end sections, indicating that condensation of water vapor will occur there. In the heated section, on the other hand, relative humidity is mostly lower than 100%, except for local peaks, and is generally smaller for Case 1 compared to Case 2, a result of the more intense convective mixing between vapor-poor and vapor-rich drift sections. In fact, we observe that the relative humidity in Case 1 never reaches 100% over the entire heated length of the drift, making it impossible for local condensation to occur in this scenario. For Case 2, on the other hand, the relative humidity is near or reaches 100% at the

cooler "5 HLW Long" and "5 HLW Short" waste packages at both 1000 and 2000 years after emplacement. Note that the local peaks in relative humidity are not a result of vapor concentration differences (which are minor according to Figure 6), but are mostly caused by the local temperature drops near the cooler waste packages.
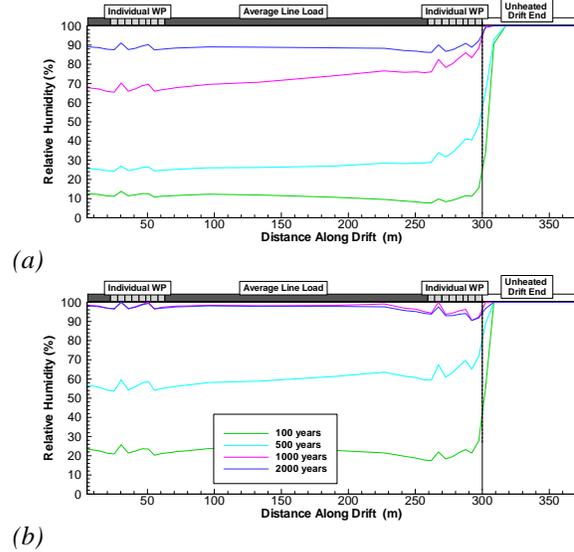

(a)

(b)

Figure 7. Relative humidity along drift crown for (a) Case 1 and (b) Case 2.

We now analyze the magnitude and evolution of condensation in the drifts. We do this by plotting the amount of liquid water that leaves the drift at the bottom and drains out into the permeable fracture network. Because there is no seepage of liquid water from the formation into the drift because of capillary forces, any water leaving the drift must be condensate that has entered in the form of vapor. We start by integrating the liquid fluxes draining out of the unheated end section of the drifts and plotting them as a function of time in Figure 8. To allow for a direct comparison, the integrated liquid fluxes leaving the drift are given as relative values, divided by the total flux arriving over the footprint of the heated drift section from ambient percolation. A relative vapor flux of one, for example, means that the vapor mass migrating from the formation into the drift is identical to the liquid mass arriving via percolation.

We can observe that for Case 1, the initial condensate flux leaving at the unheated drift end is about 10 times the percolation flux arriving over the drift footprint. This large amount of condensate stems from vaporization of resident pore water in the surrounding rock. At later times, when temperatures have returned below the boiling point, pore water evaporation is less significant. The flux reduces to relative values around 1, nearly the same as the arriving percolation flux. The sharp decline of the liquid flux around year

600 for both cases is caused by increased infiltration at Yucca Mountain, a result of an assumed climate change to monsoon conditions. Note that in the moderate convective mixing case (Case 2), the relative liquid fluxes are much smaller than what we observe in the strong convective mixing case. Initially being around 5 times the ambient percolation flux, the condensate liquid flux is less than 10% of the ambient percolation at year 2000. Because natural convection is less effective in Case 2, the amount of vapor transported along the drift is reduced compared to Case 1, and less condensate is thus deposited in the drift end section.
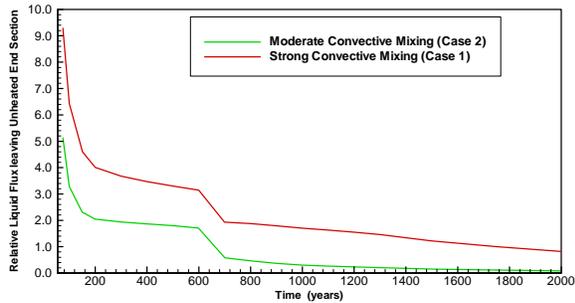

Figure 8.   Relative liquid flux leaving unheated end section of the drift for both cases.

In Figure 9, we conduct a similar evaluation of condensate flux out of the drift bottom, but this time for specific segments along the emplacement section of the drift. Like in Figure 8, fluxes are given relative to the percolation flux arriving over the footprint of the drift. Because of the vicinity to the waste packages, the existence of water in these segments is a concern to the performance of the repository. In Case 2, condensation occurs in the drift segments containing the "5 HLW Long" and "5 HLW Short" waste packages at both center and end drift locations. The maximum fluxes achieved are only 1-2% of the incoming percolation flux, indicating that almost all of the water vapor condenses in the unheated drift ends. In Case 1, liquid flux from condensate is never observed at any time in any segment of the heated drift. This was already evident from Figure 6, since relative humidity never reaches 100%. The strong convective mixing in Case 1 moves water vapor to the drift end effectively enough to never allow for condensation.

Figure 9 indicates that local condensation is a transient process that differs between center and end sections of the drift. Condensation is first observed in the cool waste packages at the drift end (starting at 600 years) where the temperatures are generally lower and below-boiling conditions exist sooner than in the center. At later times, the drift center temperatures also cool to below boiling, resulting in condensation there (starting at 900 years). The magnitude of local condensation reaches a maximum and then decreases slowly with time. Condensation eventually ceases in all cases except for the coolest "5 HLW Long" waste package in the drift center, where condensate liquid flux is still ongoing at the end of the simulation period. There are two reasons for the transient decline in the condensate liquid fluxes: (1) With less heat emanating from the waste packages, the temperature difference between hot and cold waste package segments becomes smaller. (2) With the system slowly cooling (and less evaporation of pore water occurring), less moisture is transported from the formation into and along the drifts. Overall, the period of condensation for the drift-end waste packages is earlier and less extended than for the drift-center waste packages. Note that in both locations, center or end, the magnitude of the fluxes from the "5 HLW Long" segments is larger than what is observed from the "5 HLW Short" segments. The difference here is not overall location of the waste packages along the drift but rather the smaller decay heat output from the "5 HLW Long" waste package and the resulting lower temperature at the drift wall.
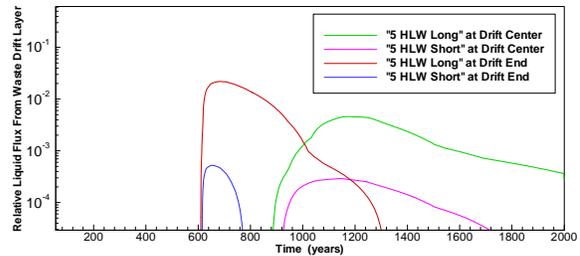

Figure 9.   Evolution of relative liquid flux from waste package segments for Case 2.

Notice the initially steep increase in condensate liquid flux for the drift-end waste packages at about 600 years. Two significant changes are introduced into the simulation at this time, both of which could contribute to trigger sudden condensation: (1) an increased infiltration flux representing future climate changes and (2) an instantaneous decrease in the vapor mass dispersion coefficient for Case 2 as given in Table 1. An increase in infiltration provides more moisture in the near-drift formation, which would then increase the amount of vapor transfer into the drift. A decrease in the effective mass dispersion coefficients results in less effective axial exchange between vapor-rich and vapor-poor regions, causing an overall increase in moisture along the heat drift sections. Apparently, with these changes in the thermodynamic conditions, the moist air reaches saturation in the vicinity of the cooler waste packages, resulting in relatively sudden condensation.

SUMMARY AND CONCLUSIONS

We have conducted a numerical study to evaluate how the vapor transport caused by natural convection in emplacement drifts at Yucca Mountain will affect

the TH conditions (temperature, relative humidity, condensates) near waste packages. A new TOUGH2-based simulation method was developed that couples existing model approaches for predicting heat and mass transport in the rock mass with modules that approximate in-drift convection as a binary diffusion process. Three-dimensional simulations runs were performed for a simplified geometrical representation of an emplacement drift plus surrounding fractured rock located in one of the southern panels of the repository. Two simulation cases were analyzed, representing different degrees of convective mixing in drifts as determined from CFD studies reported in the literature.

Our simulation results demonstrate the importance of in-drift natural convection. Strong convective mixing convection:

- causes considerable transport of vapor from heated drift sections to unheated end sections,
- gives rise to reduced relative humidity near waste packages, and
- limits the potential for local condensation near cool waste packages.

These natural convection effects are expected to improve the performance of the repository, since reduced local condensation tends to form a more desirable waste package environment. However, there are strong differences between the two simulation cases representing strong versus moderate convective mixing. The latter case predicts local condensation to occur near cool waste packages over an extended time period. In contrast, local condensation does not occur in the former case, as strong convective mixing results in favorable relative humidity conditions. Considering these significant differences, we suggest that additional CFD modeling work and scaled laboratory experiments could better constrain the effects of natural convection and condensation in Yucca Mountain emplacement drifts.

While the results of our study have demonstrated the importance of natural convection in assessing the future TH conditions in Yucca Mountain drifts, it is important to consider that we have employed several limiting model assumptions that are valid for a comparative evaluation of natural-convection sensitivity cases, but may not allow for a realistic quantitative representation. Among these are the approximation of in-drift flow patterns as a diffusive mixing process, the geometric simplification of the waste package and the drip shield as one lumped entity, and the relative coarseness of the in-drift discretization. Because of the latter, the model does not predict patterns of relative humidity conditions below the resolution of one waste package.

REFERENCES

Birkholzer, J.T., S. Mukhopadhyay, Y.W. Tsang, "Modeling Seepage into Heated Waste Emplacement Tunnels in Unsaturated Fractured Rock," *Vadose Zone Journal*, 3, 819–836, 2004.

Birkholzer, J.T., S.W. Webb, N. Halecky, P.F. Peterson, G.S. Bodvarsson, "Evaluating the Moisture Conditions in the Fractured Rock at Yucca Mountain: The Impact of Natural Convection Processes in Heated Emplacement Drifts," LBNL-59334, Berkeley, California, 2005.

Birkholzer, J.T., N. Halecky, S.W. Webb, P.F. Peterson, G.S. Bodvarsson, "The Impact of Natural Convection on Near-Field TH Processes in the Fractured Rock at Yucca Mountain," Proceedings 2006 IHLRWM Conference, Las Vegas, May, 2006.

BSC, Repository Design Project, IED Typical Waste package Components Assembly, 800-IED-WIS0-00203-000-00B, Las Vegas, NE, Bechtel SAIC Company, 2003.

BSC, "Multiscale Thermohydrologic Model," ANL-EBS-MD-000049 REV 03, Yucca Mountain Project Report, Bechtel SAIC Company, Las Vegas, Nevada, 2005.

Haukwa, C.B., Y.W. Tsang, Y.-S. Wu, G.S. Bodvarsson, "Effect of Heterogeneity on the Potential for Liquid Seepage into Heated Emplacement Drifts of the Potential Repository," *Journal of Contaminant Hydrology*, 62–63, 509–527, 2003.

Pruess, K., C. Oldenburg, G. Moridis, "TOUGH2 User's Guide, Version 2.0," LBNL-43134, Berkeley, California, 1999.

BSC, "Ventilation Model and Analysis Report," ANL-EBS-MD-000030 REV 04, Yucca Mountain Project Report, Bechtel SAIC Company, Las Vegas, Nevada, 2004.

Webb, S.W., and M.T. Itamura, "Calculation of Post-Closure Natural Convection Heat and Mass Transfer in Yucca Mountain Drifts," Proceedings of 2004 ASME Heat Transfer/Fluids Engineering Summer Conference, Charlotte, NC, June 11–15, 2004.

Webb, S.W., and A. Reed, "In-Drift Natural Convection and Condensation," MDL-EBS-MD-000001 REV 00, Yucca Mountain Project Report, Bechtel SAIC Company, Las Vegas, Nevada, 2004.